Optimising Known Transition Metal Electrocatalysts on Au Electrode by Evaluating Oxygen Evolution Reaction Kinetics and Electrocatalytic Performance in Alkaline pH

Isha Toshniwal

Under the direction of
Dr Chinmoy Ranjan
Ms Poonam
Inorganic Physical Chemistry Department
Indian Institute of Science

Research Science Initiative India July 22nd, 2025

Abstract

The persistent kinetic bottleneck associated with the anodic half-reaction in alkaline water electrolysis necessitates the development of optimized electrocatalysts. To provide superior performance, these must operate at reduced overpotentials while maintaining structural integrity under oxidative bias. Herein, we report the design and characterization of a hybrid electrocatalytic system comprising Au cores conformally coated with sub-nanometric cobalt domains. This hybrid interface facilitates significant modulation of interfacial charge distribution and electronic energy band alignment, resulting in improved OER kinetics. Catalysts were synthesised using chemical deposition, yielding discrete Co clusters on Au nanostructures immobilized on conductive supports. Electrochemical characterisation Cyclic Voltammetry, Linear Sweep Voltammetry, via Chronoamperometry revealed a striking anodic shift in the Tafel region and a reduction in the overpotential by ~ 600 mV relative to bare Au at 10 mA cm⁻², underscoring the kinetic superiority of the Au-Co heterointerface. Operando Raman spectroscopy was employed to probe potential dependent lattice restructuring, analyse the surface morphology and composition of both electrocatalysts. The emergence of vibrational signatures in the 570-600 cm⁻¹ region and a distinct high-frequency mode at ~810 cm⁻¹, attributable to O-O stretching in surface-bound cobalt oxyhydroxide intermediates, correlates with the onset of catalytic activity and confirms oxidative rehybridization of the Co domain. These findings suggest that synergistic d-band coupling at the Au-Co interface and the presence of spatially localized electric fields amplify reaction rates, while also stabilizing high-valent CoOx species. The Au-Co hybrid electrocatalyst presents a compelling blueprint for the design of multi-component, transition metal electrocatalysts that achieve high OER activity through phase-selective surface reconstruction and electronic coherence across a metal-metal oxide junction.

Summary

Producing hydrogen by splitting water is a promising way to generate and store clean energy, but the process faces a major hurdle. The oxygen evolution reaction (OER), is slow and requires a large amount of energy. To make this step more efficient, scientists are constantly looking for better materials, namely electrocatalysts, that can speed up the reaction without falling apart under different stresses. In this study, we developed a novel catalyst composition by combining gold (Au) with cobalt (Co) at the nanoscale. Gold is known for its ability to interact with light and electrons in useful ways, yet it is not an efficient OER catalyst. Cobalt, on the other hand, is an active transition metal that can undergo useful chemical changes under electric current. By coating gold particles with an ultra-thin layer of cobalt, we created a hybrid material that performs much better than gold alone. To understand the surface composition of this electrocatalyst, we used a special technique called operando Raman spectroscopy, which lets us watch how the material's surface changes in real time during the reaction. Raman signals suggested the formation of active cobalt-based compounds as the reaction began, showing that the material adapts and reorganizes to become more active under operating conditions.

1 Introduction

The global energy transition demands sustainable, scalable solutions to decarbonize sectors ranging from transportation to industry [1]. One of the proven technologies to generate green hydrogen and pure oxygen is water electrolysis, yet the problem arises in finding sustainable energy inputs. Hydrogen is a clean, high energy density fuel that produces water as its only byproduct, making it useful in future energy systems [1]. However, the efficiency and durability of water electrolyzers hinges on the development of high performance electrocatalysts for Hydrogen Evolution Reactions (HER) and the Oxygen Evolution Reactions (OER) [2]. While OER catalysts such as Iridium Oxide and Ruthenium(IV) Oxide show high stability, their scarcity and cost severely limit scalability [2]. This has driven the exploration of alternative electrocatalysts, including those based on transition metals, carbon, or metal oxides. Noble metals like gold remain crucial for their surface and structural stability, which make them ideal systems to study fundamental electrocatalytic behavior [2]. Particularly, understanding how cobalt deposition on gold electrodes impact OER kinetics and active site activity will be used to offer insights into optimizing catalytic performance in an alkaline environment. This study explores how cobalt (Co), a known transition metal OER catalyst [35], behaves when deposited on electrochemically treated Au surfaces. An electrocatalyst is an interface through which an electrochemical reaction, in which chemical energy is converted into electrical energy in fuel cells occurs [3]. They provide active sites for the reaction which facilitate electron and ion transfer, stabilize reaction intermediates, and operate efficiently under electrochemical conditions.

1.1 Electrocatalysts and their effect on reaction dynamics

The aforementioned water electrolysis process involves applying an electrical potential across two electrodes submerged in an electrolyte, causing water to split into hydrogen and oxygen gases. This process comprises two half-reactions, each occurring at a separate electrode [1]. At the cathode, HER occurs. In an alkaline medium, it is: [4,5]

$$2H_2O + 2e^- \rightarrow H_2 + 2OH^-$$
 Equation 1

The OER must be catalyzed efficiently to minimize the overpotential, i.e. the extra voltage beyond the theoretical requirement (1.23 V vs. Reversible Hydrogen Electrode) which is needed to drive the reaction (See Appendix A.1 for more detail). The OER is also necessary to complete the circuit and balance electron flow in the electrochemical cell [4]. In the alkaline medium:

$$4OH^- \rightarrow 2H_2O + 4e^- + O_2$$
 Equation 2

Since OER is a four-electron process involving complex intermediate steps such as *OH, *O, *OOH [6], it is slow and kinetically demanding. Hence, it usually requires a higher overpotential than HER and leads to significant energy loss. To reduce these overpotentials, an electrocatalyst is needed [7]. Fuel cell efficiency largely depends on the electrocatalyst. While metal-based catalysts are common, they often lack durability and pose environmental concerns. Thus, there is a growing need for stable, low-cost, and

eco-friendly transition metal alternatives [3, 8]. A highly active catalyst can achieve a high current density with minimal energy input [1]. A stable electrocatalyst should maintain its performance over long-term electrolysis, resisting physical, chemical, or structural changes that would otherwise reduce its effectiveness [15].

1.2 Choosing materials for electrocatalysts

Plasmonic metals such as gold are used as electrocatalysts due to their high chemical stability, well-defined surface structure, and ability to form tunable surface oxides that modify its catalytic behavior [24]. Although it does not produce the largest recorded current i.e. it is not the most active metal for OER/HER reactions, gold offers high selectivity and maintains moderate binding to key intermediates. Hence, Au prevents surface poisoning [25], which is the adsorption of impurities onto the catalyst surface thus deactivating the catalyst by blocking active sites. Being inert makes gold ideal for studying the OER. Even when the gold core is fully covered by a cobalt-based overlayer as it is in the Au-Co electrocatalyst, its surface properties remain critically important due to strong electronic and interfacial interactions. Specifically, gold can donate or withdraw charge from the cobalt overlayer, shifting its electronic structure through interfacial charge transfer and modifying the band alignment between the two metals. Such interactions can widen the d-band of the cobalt layer, a phenomenon that directly affects the binding strength of OER intermediates like *OH, *O, and *OOH. A d-band center that is neither too high (causing overbinding) nor too low (causing underbinding) is critical for optimal catalytic turnover. Additionally, the Au-Co interface often serves as a catalytic hotspot, especially at grain boundaries or pinholes where the gold may be partially exposed or electronically coupled. Gold's high conductivity and chemical stability also contribute to the structural integrity of the hybrid catalyst, preventing dissolution or degradation of cobalt species under high anodic bias.

Cobalt itself is a highly promising OER catalyst in alkaline media due to its favorable redox behavior and ability to form electroactive species like $Co(OH)_2$, CoOOH, and Co_3O_4 under anodic potentials. It is electrodeposited onto the Au substrate, allowing precise control over film thickness, morphology, and composition. The hybridization of Au and Co results in synergistic effects, where the overall catalytic performance of the composite exceeds the sum of its parts. Additionally, the presence of Au can modulate the oxidation state transitions in cobalt such as Co^{2+}/Co^{3+} or Co^{3+}/Co^{4+} , making the formation of catalytically active CoOOH phases more favorable.

We compared Au-CoOx to pure Au and not to pure Co to specifically isolate and evaluate the synergistic effect of cobalt oxide functionalization on a noble metal substrate. Gold (Au) serves as a chemically stable, inert, and conductive baseline, allowing us to directly attribute performance enhancements to the cobalt species deposited on its surface. Additionally, pure cobalt is prone to dissolution and surface degradation under OER conditions, whereas Au provides a stable platform for studying the intrinsic activity of cobalt-based active sites without significant interference from substrate degradation.

In sum, the Au-Co system exemplifies how hybrid interfaces can be engineered to optimize charge transfer, intermediate binding energy, and structural stability, ultimately improving OER kinetics.

2 Method

To evaluate parameters like onset potential, overpotential, Tafel slope, charge transfer resistance, and long-term stability, a set of standardized electrochemical techniques are employed: cyclic voltammetry (CV), linear sweep voltammetry (LSV), chronoamperometry (CA), and electrochemical impedance spectroscopy (zero impedance resistance) (See Appendix A for more detail). The as-synthesized material was characterized to evaluate its morphology (See Appendix E.1 for more detail) and composition with Raman spectroscopy. We focus on Surface Enhanced Raman Spectroscopy as our primary material evaluation and characterization method. It is an in situ technique that detects catalyst phase transitions [36], such as oxidation, intermediate formation, and surface reconstruction, and can be integrated with electrochemical cells to directly link spectral changes with applied potential, current, and reaction kinetics [37]. Raman works well with metal oxides, hydroxides, phosphides, and sulfides – unlike other spectrometers which focus on organic functional groups – that are commonly used in the analysis of HER and OER catalysts. (See Appendix B for more detail).

2.1 Synthesis and evaluation of catalyst

A two electrode set up was used for the electrodeposition of the Co catalyst on Au. A standard polycrystalline Au electrode was used as the working electrode while Pt wire was used as the counter electrode. Before the electrodeposition process was carried out, the Au electrode was cleaned electrochemically in $0.1~\rm M~H_2SO_4$ by employing cyclic voltammetry. A precursor solution was prepared from $0.1~\rm M~Co(NO_3)_2.6H_2O$, using the ultrapure water with resistivity 18 M Ω ·cm. The deposition of Co was conducted using chronopotentiometry. After the preparation of the catalyst, its activity was evaluated in a three electrode setup. Ag/AgCl (Satd. KCl) was used as the reference electrode.

LSV and CA techniques were used to test the samples catalytic activity in 1 M NaOH electrolyte using a Biologic VSP Potentiostat/Galvanostat. The obtained voltammograms are reported with respect to Reversible Hydrogen Electrodes (RHE). The conversion of electrode potential of Ag/AgCl (Satd. KCl) to RHE is performed by the following equation [32].

$$E_{RHE} = E_{measured} + E_{ref}^{\circ} + 0.0591 \times pH$$
 Equation 3

2.2 CV, LSV, CA, CP parameters for testing and synthesis

Multiple different tests were employed on the Au electrode. Cyclic voltammetry (to observe HER and OER activity) was conducted from 0.5 to 2.3V vs RHE for 15 seconds at a

scan rate of 50 mV/s. Linear sweep voltammetry (redox activity) was carried out from 1.54 to 2.3V vs RHE at a scan rate of 4 mV/s.

Chronoamperometry (See Appendix C for more detail) was conducted from 1.5 to 2.26V vs RHE with 0.04V increments, each for 2 minutes. Open circuit voltage (the pre-existent potential difference between both electrodes) was calculated to assess preliminary potential between working and reference electrodes. pH was maintained at 14 for all performance assessments by using 99% pure 1 M NaOH solution.

The catalyst surface was rinsed in Millipore water to remove unbound species and dried with argon gas. Once the Au-Co surface was prepared, CV at 100 mV/s, LSV at 4 mV/s and CA (with 0.04 V gap for 2 minutes each) were conducted from 0.85 to 1.65V.

Tafel analysis was carried out in the kinetically controlled regime of the polarization curves to determine the Tafel slope and infer mechanistic details. The as-prepared Co-Au catalyst was characterized with Raman spectroscopy. The Raman spectra were recorded on a Renishaw In-Via Raman Microscope with a 785 nm excitation wavelength, coupled to a Leica DM 2700 microscope.

3 Results

3.1 Chronopotentiometry for catalyst deposition

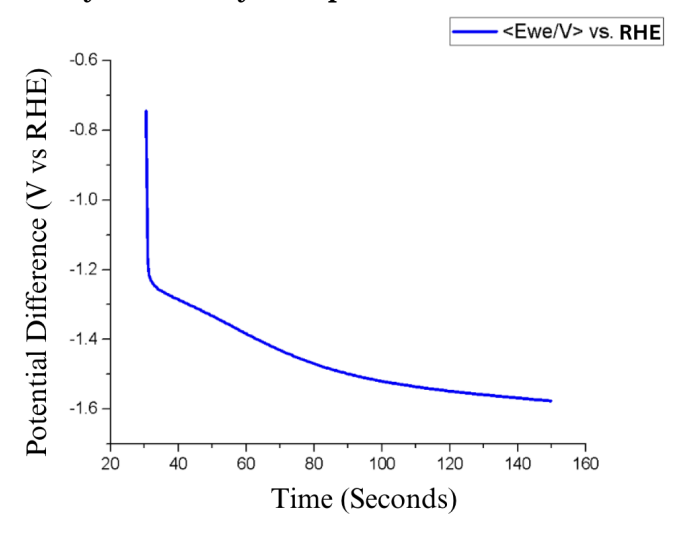


Figure 1 Electrodeposition of Cobalt film on the Au electrode was conducted using 0.1 M cobalt nitrate solution by using chronopotentiometry at -0.7 mA for 2 minutes.

In figure 1, stable deposition of cobalt on the gold substrate was observed. The relatively L-shaped curve with less noisy deposition showcases successful electrodeposition and formation of the hybrid catalyst. This deposition is done by applying a constant potential (-0.7 mA) while using $Co(NO_3)_2$ as the electrolyte in order to deposit Co on the Au substrate and form the hybrid catalyst. The graphical observation is a lab standard for deposition.

3.2 Cyclic Voltammetry Studies on Au and Au-Co surfaces

To probe the redox behavior and electrocatalytic activity of the synthesized catalysts, cyclic voltammetry (CV) was performed in aqueous 1 M NaOH electrolyte.

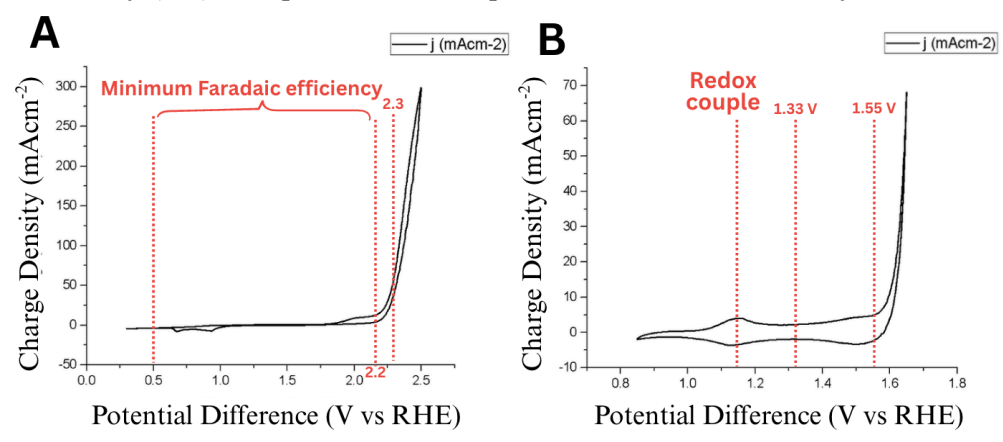


Figure 2 (A) Cyclic Voltammogram (CV) of the Au surface at scan rate 100 mV/s from 0.5 to 2.28 V vs RHE. (B) CV profile of Au-Co surface at scan rate 100 mV/s from 0.85 to 1.65 V vs RHE. Measuring current density (j) against potential (V). This data represents the OER i.e. large positive tail of the voltammogram and displays redox activity of the catalysts.

The Au catalyst (Figure 2A) exhibits minimal faradaic activity from 0.5 to ~ 2.2 V vs RHE [39]. This is followed by a gradual rise in anodic current corresponding to the formation of gold oxide (AuOx) species. A steep current increase is observed beyond ~ 2.3 V vs RHE, attributable to the onset of the oxygen evolution reaction (OER). This high (when compared to Au-Co) OER onset potential confirms the inherently poor OER kinetics of gold, consistent with its weak interaction with oxygenated intermediates. In contrast, the Au-Co (Figure 2B) surface displays a distinct pair of redox peaks centered around 1.15-1.33 V vs RHE. These features are assigned to the $\mathrm{Co^{2+}}$ / $\mathrm{Co^{3+}}$ redox couple, indicating the presence of electrochemically active cobalt species. The oxidation peak at ~ 1.33 V corresponds to the formation of CoOOH from $\mathrm{Co}(\mathrm{OH})_2$, a key intermediate in the OER pathway.

In Figure 2B, the reduction peak at ~1.15 V reflects the quasi-reversible nature of this transition. Notably, OER onset occurs at a lower potential (1.55 V) with a sharper increase in current which confirms enhanced catalytic activity upon Co introduction. These results underscore the synergistic effect between gold and cobalt, where gold provides a conductive and stable scaffold, while cobalt contributes active redox centers. Although the overall current density in the Au-Co voltammogram (Figure 2B) is lower due to a narrower potential range, the emergence of redox peaks and the earlier onset of OER suggest improved surface kinetics compared to bare Au. These features indicate the formation of cobalt-based intermediates and a reduced activation barrier for water oxidation. The presence of cobalt clearly improves the surface kinetics for water oxidation, as evidenced by both the emergence of redox activity and a lower OER overpotential compared to pure Au.

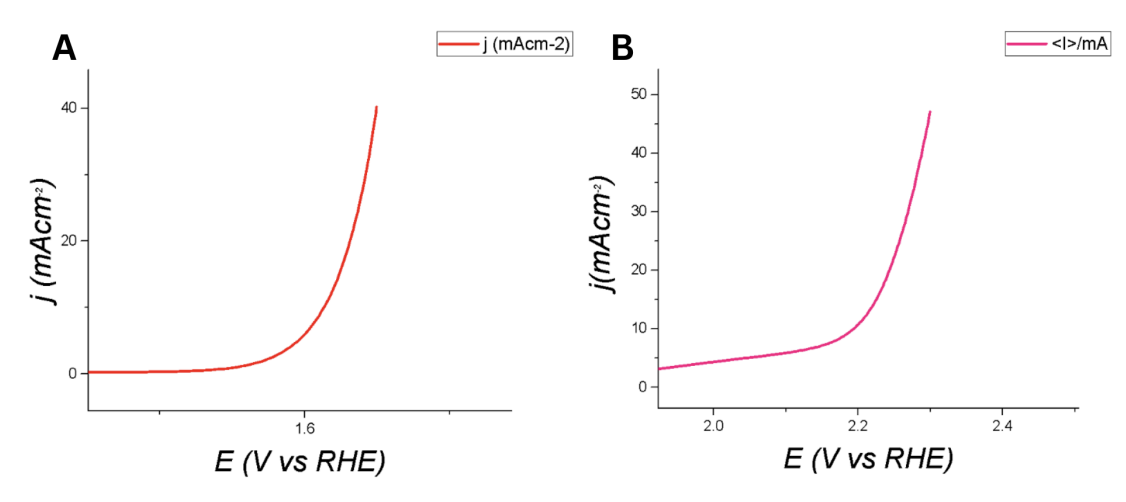


Figure 3 (A) Linear Sweep Voltammetry (LSV) for pure Au substrate from 1.54 to 2.28 V vs RHE. This shows the catalytic activity of pure Au in this range. (B) LSV for Au-Co from 0.85 to 1.65 V vs RHE, displaying activity of Au-Co in this voltage range. The potential ranges were optimised after trial and error in order to select voltages where high activity was observed. The test is conducted in order to test catalytic activity and prove the catalyst is working in alkaline conditions.

3.3 α-Au and β-Au Oxide Formation

In the CV profile of pure gold (Figure 2A), a sharp increase in current density is only observed beyond ~2.3 V vs RHE, corresponding to the onset of the oxygen evolution reaction (OER). This high overpotential and lack of redox features are consistent with the literature-reported sequential oxidation of gold [26], wherein a thin α -AuOx (likely Au₂O) layer forms at lower potentials without significantly enhancing catalytic activity. As the potential approaches 2.3 V, the formation of a thicker and more resistive β -AuOx (Au₂O₃) phase likely dominates, further passivating the surface. The accumulation of these oxide layers inhibits electron transfer and active site accessibility, leading to delayed and inefficient OER onset with both high overpotential and low current output.

In contrast, the CV of the Au-Co system (Figure 2B) shows a marked improvement in electrochemical behavior. A pair of redox peaks is observed, with the oxidation peak at ~1.33 V and the reduction peak at ~1.15 V vs RHE, corresponding to the quasi-reversible $\text{Co}^{2^+}/\text{Co}^{3^+}$ redox couple. These features indicate the presence of electrochemically active cobalt species capable of participating in OER-relevant transformations such as $\text{Co}(\text{OH})_2$ to CoOOH. More importantly, a pronounced increase in current begins at a much lower potential of ~1.55 V, confirming earlier OER onset and improved kinetics. This enhancement is attributed not only to the catalytic activity of Co redox centers but also to their influence on the gold surface. Cobalt incorporation may stabilize a thinner α -AuOx layer while suppressing the transition to β -AuOx, thereby maintaining better surface conductivity and catalytic accessibility.

Overall, the comparative CVs highlight the detrimental impact of thick β -AuOx accumulation on pure Au and the synergistic benefits of Co addition in modulating oxide chemistry and facilitating more efficient OER.

3.4 Chronoamperometry on Au and Au-Co surface for OER

The performance of electrocatalysts in the oxygen evolution reaction (OER) is dependent on the overpotential (η) required to reach a benchmark current density, typically set at 10 mA cm⁻², which is the current density obtained in a 10 % efficient solar water splitting device. In this study, chronoamperometry (CA) was employed to determine the potential at which each catalyst achieves this current density, thereby allowing for direct comparison of catalytic efficiency between the Au-Co hybrid surface and the Au surface.

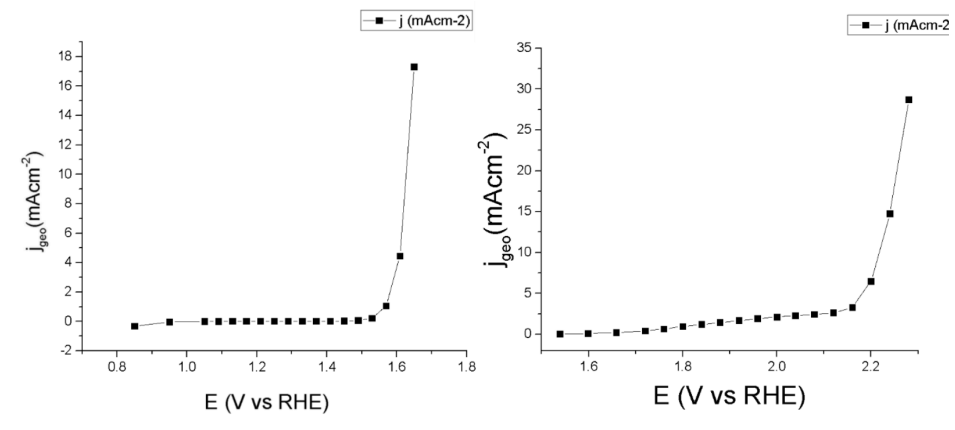


Figure 4 illustrates chronopotentiometry, displaying the current density (j) as a function of applied potential (E vs RHE): (A) Chronoamperometry of Au-Co catalyst which displays an onset of rapid current increase beyond ~1.5 V, reaching the standard 10 mA cm⁻² current density at 1.627 V vs RHE. (B) Chronoamperometry of Pure Au surface showing a more gradual increase in current density, achieving 10 mA cm⁻² at a significantly higher potential of 2.219 V vs RHE. Scale is not normalised.

To quantitatively assess catalytic efficiency, the overpotential (η) was determined by subtracting the thermodynamic equilibrium potential for water oxidation (1.23 V vs RHE) from the experimentally measured potential at 10 mA cm⁻². Thus, for Au-Co, $\eta=398$ mV, and for Au, $\eta=989$ mV. A lower overpotential corresponds to a more efficient electrocatalyst, as less additional potential (beyond the thermodynamic minimum) is required to drive the OER. The nearly 600 mV overpotential between the Au-Co and Au catalysts indicates enhanced catalytic activity in the Au-Co system. Such a large shift indicates that Co incorporation reduces the kinetic barrier for O_2 evolution. Traditionally, a 50-100 mV decrease in overpotential upon electrodepositing Ir or Pi on Au is considered significant when optimizing OER catalysts [40]; therefore, a 600 mV drop suggests that our deposition parameters form an ideal surface for OER with performance six fold better than recorded literature. For future scope, exploring the precise potential windows and conditions (pH, scan rate) that optimize the α -oxide layer while minimizing β -oxide formation could enhance gold's catalytic efficiency.

The improved performance of the Au-Co surface may be attributed to synergistic interactions between gold and cobalt atoms at the catalyst interface. Cobalt facilitates the adsorption and deprotonation of water molecules, thereby accelerating OER intermediates'

formation. Gold, while generally inert for OER, provides electronic conductivity and structural stability; and in configurations such as sub-monolayer Co deposition, gold may modulate the electronic environment of active Co sites. This synergism could lower the energy barrier for the formation of OER intermediates on the surface, resulting in a lower overpotential. Furthermore, the enhanced current response of the Au-Co catalyst in the 1.4-1.65 V region suggests rapid charge transfer kinetics and favorable surface hydrophilicity which is critical in sustaining water oxidation reactions.

The delayed current onset and the steeper slope in the CA curve in Figure 4B reinforce the limited ability of the Au surface to facilitate the multi-electron transfer steps involved in OER, even at elevated potentials. Additionally, the high overpotential may cause unwanted side reactions or material degradation, thereby limiting the long-term viability of Au as a standalone electrocatalyst.

3.5 Tafel Analysis

To evaluate the oxygen evolution reaction (OER) kinetics of the synthesized catalysts, Tafel slopes were extracted from chronoamperometry (CA) data for both electrocatalysts.

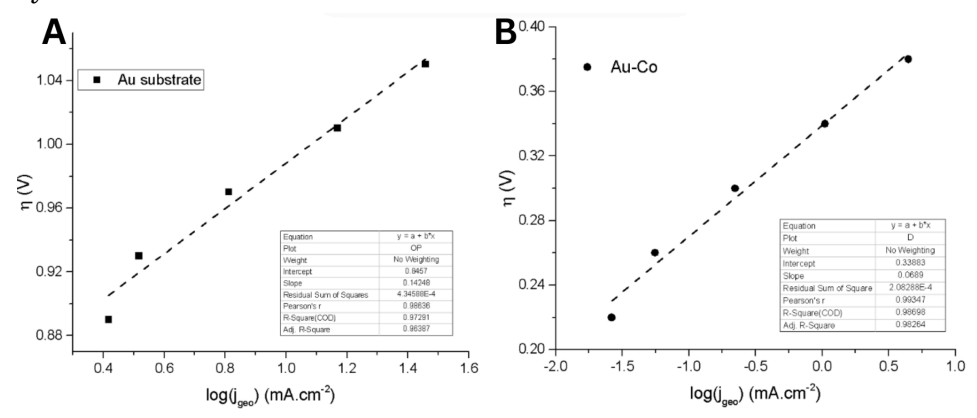


Figure 5 (A) Tafel plot for pure Au surface within 2.12-2.28 V vs RHE. (B) Tafel plot for Au-Co surface from 1.41-1.61 V vs RHE. A Tafel plot shows reaction kinetics by illustrating how the overpotential (η) – the extra voltage needed to drive a reaction – changes with logarithmic current density (log j). Since current density reflects the rate at which electrons are transferred during the electrochemical reaction, the slope of the plot (the Tafel slope) reveals how efficiently a catalyst facilitates that charge transfer. Scale is not normalised.

A low tafel slope indicates an active catalyst as a smaller overpotential required to increase the current density by one order of magnitude.

Figure 5(A) displays a high tafel slope for Au substrate 142 mV dec⁻¹. This value lies within the typical range observed for efficient OER catalysts and indicates sluggish reaction kinetics, likely governed by a rate-determining step involving sluggish charge transfer or limited *OH/*O intermediate formation. Figure 5(B), in contrast, shows a much lower Tafel slope of 68.9 mV dec⁻¹ for the Au-Co surface in the range of 1.41 – 1.61 V vs RHE. This value lies within the expected range for oxygen evolution reaction pathways, particularly in

alkaline media, and is indicative of significantly improved kinetics. The high linearity (adjusted $R^2 = 0.98$) of the recorded measurements reflects consistent and stable catalytic behavior. From Figure 5A, the high Tafel slope could also indicate possible surface passivation by thick β -AuOx layers, as supported by earlier CV data. The deviation from ideality (adjusted $R^2 = 0.96$) is low. These findings are consistent with gold's known inertness and weak adsorption of OER intermediates, which necessitate a high overpotential to drive the reaction forward. The difference between Tafel slopes observed is attributed to the synergistic effect of cobalt, which introduces redox-active sites and may modulate oxide layer formation on Au to suppress the inactive β -phase while stabilizing a more conductive α -AuOx. These results, together with CV data showing earlier onset and higher current density, confirm that the Au-Co hybrid substantially outperforms pure Au in facilitating the OER. (See Appendix D for more detail).

3.6 Raman Analysis

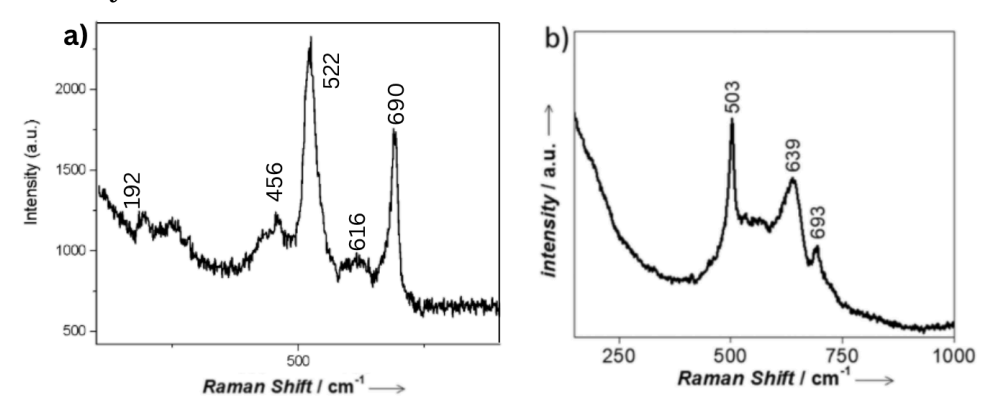


Figure 5 Raman Spectra of CoOx/Au sample before and after immersion in the NaOH electrolyte. a) CoOx/Au - as prepared (i.e. spectra captured immediately after preparation). b) CoOx/Au sample upon immersion for 15 minutes, Raman spectra collected in the electrolyte in order to show stable properties of Au/CoOx.

Panel A of Figure 5 presents the Raman spectrum of the catalyst immediately post preparation, displaying multiple well-defined vibrational bands that reflect the coexistence of various cobalt-based species and surface adsorbates. Notably, sharp peaks at 456 cm⁻¹ and 522 cm⁻¹ are attributed to the vibrational modes of Co(OH)₂, indicating the presence of cobalt hydroxide phases often associated with initial electrodeposition or hydration. The intense bands at 192 cm⁻¹ and 690 cm⁻¹ correspond to the F₂g and A₁g modes of Co₃O₄, respectively, confirming the presence of a mixed-valence spinel structure (Co²⁺/Co³⁺), which is often observed in cobalt-based catalysts prior to electrochemical activation. A broad peak centered at 616 cm⁻¹ is characteristic of CoOOH, a Co³⁺ rich oxyhydroxide phase that typically forms during oxidative preconditioning and plays a central role in active oxygen evolution reaction (OER) catalysis. The strong band at 1053 cm⁻¹ is assigned to the symmetric stretching vibration (v₁) of NO₃⁻, suggesting the retention of residual nitrate ions from the cobalt precursor salts. Additionally, the peak at 952 cm⁻¹ is indicative of SO₄²⁻

species, likely arising from trace sulfates from washing steps or ambient contamination. Overall, the spectrum captures a transition zone between inactive hydroxide and mixed-valence oxide species such as $Co(OH)_2$ and Co_3O_4 and active CoOOH domains, marking the initial stages of oxidative rehybridization and catalyst surface evolution prior to OER onset.

The Raman spectra was obtained when the as-prepared CoOx/Au was submerged in aqueous 1 M NaOH electrolyte [39] and is displayed in Figure 6(b). It displays multiple well-resolved bands associated with cobalt-based oxide and oxyhydroxide phases. This indicates the material transformation occurs and stable oxide and hydroxide phases of cobalt were formed which are stable in 1 m NaOH solution. The peaks at 639 and 693 cm⁻¹ correspond to the A_{1g} stretching modes of Co–O in Co_3O_4 , indicative of the spinel cobalt oxide structure containing both Co^{2+} and Co^{3+} species. Notably, the peak at 503 cm⁻¹ is characteristic of CoOOH, which is rich in Co^{3+} and emerges during initial electrochemical exposure of the species.

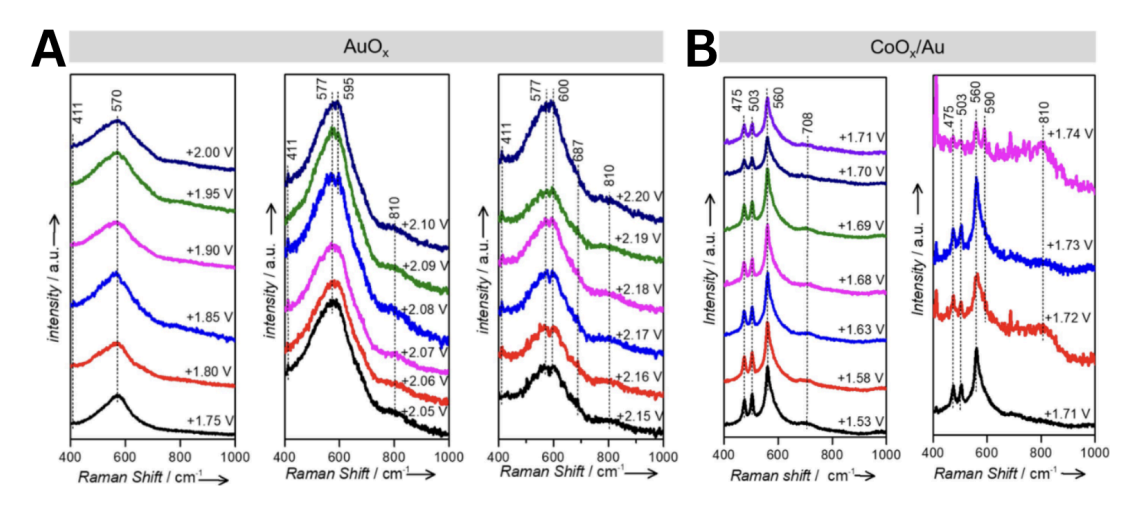


Figure 6 In situ Raman spectroscopy for Au surface during OER to form AuOx. 0.1V steps used between measurements. Image obtained from [39]

Operando Raman spectroscopy (Figure 6) monitored the progressive surface oxidation and identified key intermediates during oxygen evolution reactions (OER) on both AuO_x and CoO_x/Au electrodes under alkaline conditions [39]. For the AuO_x system, spectra collected between +1.75 V and +2.20 V vs RHE reveal gradual development of vibrational features associated with gold oxide formation. At lower potentials (1.75–1.90 V), weak, broad bands near ~570 cm⁻¹ and a shoulder at ~411 cm⁻¹ emerge, corresponding to vibrational modes of disordered or hydrated AuOx species. As the potential increases beyond +2.05 V, peaks at 577 cm⁻¹ and 595 cm⁻¹ become more prominent, indicative of progressively oxidized Au phases, likely containing Au^{3+} . A distinct Raman band at ~810 cm⁻¹ appears at \geq 2.05 V, coinciding with the onset of measurable OER current on Au and corresponding to the O–O stretching vibration of *OOH type species on the gold surface.

In contrast, the ${\rm CoO_x/Au}$ hybrid system displays markedly different behavior. With Raman spectra acquired between +1.53 V and +1.74 V vs RHE showing early formation of catalytically relevant cobalt oxide phases. Well-defined peaks at ~400 cm⁻¹, ~475 cm⁻¹, ~503 cm⁻¹, ~560 cm⁻¹, and ~590 cm⁻¹ emerge and intensify with increasing potential. The 503 cm⁻¹ peak is attributed to ${\rm CoOOH}$, a redox-active cobalt oxyhydroxide. The 475 cm⁻¹ and 560 cm⁻¹ peaks correspond to ${\rm CoO_2}$ type layered oxides containing mixed ${\rm Co^{3+}/Co^{4+}}$ states, and the 590 cm⁻¹ band likely arises from lattice vibrational modes of activated cobalt oxide (${\rm CoO_2}$) structures. Notably, the ~810 cm⁻¹ band, indicative of O–O bond formation in adsorbed *OOH intermediates appears at +1.71 V for ${\rm CoO_x/Au}$ – substantially earlier than for pure Au – thus implying that Co incorporation facilitates key steps in the OER mechanism at significantly lower overpotentials.

The ~810 cm⁻¹ peak, which has been reported in prior literature as a peroxo-type intermediate, suggests active oxygen species formation at highly oxidizing potentials [38]. This observation aligns with electrochemical data showing a lower overpotential (600 mV) and reduced Tafel slope (69 mV dec⁻¹) for CoO_x/Au compared to Au. Since the 810 cm⁻¹ peak arises in both systems, despite their differing onset potentials, we can deduce that vibrational signature represents a shared intermediate rather than a metal specific species.

Overall, these Raman results highlight the distinct oxidation pathways of Au and CoO_x -modified Au surfaces and provide spectroscopic evidence that transition metal incorporation not only enhances catalytic activity but also modulates the surface to favor earlier and more efficient OER intermediate formation.

To contextualise our overall results and discussion, a direct comparison with the commercial Pt/C catalyst which is commonly used in water splitting setups shows that our CoOx/Au system performs better in several aspects. While both catalysts operate in the ~400 mV overpotential range [1], the *CoOx/Au surface achieves earlier formation of *OOH intermediates at 1.71V seen in the Raman spectra in Figure 6, which is a clear sign of faster OER kinetics. Moreover, Pt-based catalysts are significantly more expensive as platinum costs roughly 5 times more per gram than gold [44], and unlike cobalt, it's not earth-abundant. Pt also tends to degrade faster under alkaline conditions due to surface oxide formation and Pt dissolution, making it less suitable for long-term electrolyser use in alkaline media [45, 46]. In contrast, the CoOx/Au electrode offers a cost-effective and kinetically superior alternative, backed by real-time Raman evidence showing early activation of catalytically active cobalt oxide species.

4 Conclusion

In this study, we synthesized the catalyst in a single step by the electrodeposition technique at ambient conditions. We found that modifying the Au substrate with cobalt oxide functionalisation improves the catalytic activity in comparison to pure Au substrate. The catalytic activity of the electrocatalysts was evaluated by Linear Sweep Voltammetry. The improved catalytic activity of Au-Co catalyst was demonstrated by a lower overpotential of 398 mV compared to 989 mV for pure Au substrate. A 600 mV overpotential

reduction per cell translates to almost ~27% decrease in energy consumption for oxygen evolution in comparison to a standard electrolyser [47]. When scaled to full electrolyser systems, this can lead to lower power requirements, reduced operational costs, and higher hydrogen yields per unit of energy. Tafel slope analysis revealed the Co-modified Au catalyst has a lower tafel slope (69 mVdec⁻¹) than pure Au substrate (142 mVdec⁻¹) indicating improved OER kinetics. Operando Raman spectroscopy further revealed the formation of CoOOH-like active intermediates under anodic bias, confirming the dynamic restructuring of the catalyst surface during operation. The observed Raman peaks provide compelling evidence of the dynamic surface transformations and intermediate species that underpin the electrocatalytic performance of the Co-Au system during the oxygen evolution reaction (OER). Notably, the strong ~810 cm⁻¹ band corresponds to the O-O stretching vibration of the *OOH intermediate, a critical species in the OER pathway. The detection of *OOH signifies that the catalyst surface not only adsorbs oxygen-containing species but also actively participates in the rate-limiting O-O bond formation step. Altogether, the emergence of these peaks reflects the evolution of catalytically competent phases and intermediates, highlighting the synergistic interplay between cobalt and gold in enhancing the overall OER activity.

Quantum chemical studies provide further evidence that depositing cobalt (Co) onto a gold (Au) substrate enhances Co oxidation. These studies indicate that oxygen atoms bind more strongly to a monolayer of Co on Au compared to pure Co. This is likely due to tensile strain from the Au substrate, which raises the energy level of Co's d-band center, thereby increasing its affinity for oxygen and enhancing Co–O bond strength [42].

These findings highlight the critical role of interfacial engineering and transition metal incorporation in overcoming the kinetic limitations of noble metal catalysts. Overall, this work provides a rational strategy for designing efficient OER catalysts by leveraging the synergistic effects between conductive Au substrate and non-noble transition metals.

This study has several limitations. The use of polycrystalline gold introduces slight surface variability that was not characterized, potentially minorly affecting cobalt deposition and reactivity. Cobalt loading and distribution were also not quantified, limiting insight into active site density. While in situ Raman confirmed key phases like CoOOH and *OOH, it remains semi-quantitative and may suffer from spectral overlap or noise. The study also did not explore catalyst behavior in acidic or neutral media, which may affect broader applicability. Future work could include surface mapping (ECSA), time-resolved analysis, and durability testing.

5 Acknowledgments

I would like to humbly express my gratitude towards Dr. Chinmoy Ranjan (IISC), Ms Poonam (IISC), Mr Anthony Cheng (CMU), Dr. David Farris (IISc), Max & Aubrey Bee-Lindgren for their invaluable expertise, Dr. Amy Sillman (CEE), the Center for Excellence in Education, the Adani Group and the Indian Institute of Science without

whom this research would not be possible. I extend my heartfelt gratitude to my readers for their patience and time.

6 References

- [1] Seh, Z. W., Kibsgaard, J., Dickens, C. F., Chorkendorff, I., Nørskov, J. K., & Jaramillo, T. F. (2017). Combining theory and experiment in electrocatalysis: Insights into materials design. *Science*, 355(6321), eaad4998. https://doi.org/10.1126/science.aad4998
- [2] SZeliang Ju, Xiujuan Tan, Xuyun Zhang, Yong Wang, Chengfeng Yin, Qingxin Kang, Dual active site pathways in cobalt-based bimetallic catalysts enhance oxygen evolution reaction activity: Density functional theory studies, Surfaces and Interfaces, 2024, https://doi.org/10.1016/j.surfin.2024.105428.
- [3] Banoth, P., Kandula, C., & Kollu, P. (2022). Introduction to Electrocatalysts. In *ACS* symposium series (pp. 1–37). https://doi.org/10.1021/bk-2022-1432.ch001
- [4] Seh, Z. W., Kibsgaard, J., Dickens, C. F., Chorkendorff, I., Nørskov, J. K., & Jaramillo, T. F. (2017). Combining theory and experiment in electrocatalysis: Insights into materials design. *Science*, 355(6321), eaad4998. https://doi.org/10.1126/science.aad4998
- [5] Sheng, W., Myint, M., Chen, J. G., & Yan, Y. (2013). Correlating hydrogen evolution reaction activity in alkaline electrolytes with the hydrogen binding energy on monometallic and bimetallic catalysts. *Energy & Environmental Science*, 6, 1509–1512. https://doi.org/10.1039/C3EE00045A
- [6] Zhuang Zeng, Siyu Kuang, Zhen-Feng Huang, Xiaoyi Chen, Yaqiong Su, Yue Wang, Boosting oxygen evolution over inverse spinel Fe-Co-Mn oxide nanocubes through electronic structure engineering, Chemical Engineering Journal, 2022, https://doi.org/10.1016/j.cej.2021.134446
- [7] Man, I. C., Su, H. Y., Calle-Vallejo, F., Hansen, H. A., Martínez, J. I., Inoglu, N. G., ... & Nørskov, J. K. (2011). Universality in oxygen evolution electrocatalysis on oxide surfaces. *ChemCatChem*, 3(7), 1159–1165. https://doi.org/10.1002/cctc.201000397
- [8] Garcia-Olmo, A. J., Yepez, A., Balu, A. M., Romero, A. A., Li, Y., & Luque, R. (2016). Insights into the activity, selectivity and stability of heterogeneous catalysts in the continuous flow hydroconversion of furfural. *Catalysis Science & Technology*, 6(13), 4705–4711. https://doi.org/10.1039/c6cy00249h
- [9] Libretexts. (2023, August 4). 3.8: Day 25- Homogeneous and heterogeneous catalysis. ChemistryLibreTexts.https://chem.libretexts.org/Bookshelves/General_Chemistry/Interactive_Chemistry_(Moore_Zhou_and_Garand)/03%3A_Unit_Three/3.08%3A_Day_25-_Homogeneous_and_Heterogeneous_Catalysis
- [15] McCrory, C. C. L., Jung, S., Peters, J. C., & Jaramillo, T. F. (2013). Benchmarking heterogeneous electrocatalysts for the oxygen evolution reaction. *Journal of the American Chemical Society*, 135(45), 16977–16987. https://doi.org/10.1021/ja407115p
- [16] H. Gunaseelan, A.V. Munde, R. Patel, B.R. Sathe, Metal-organic framework derived carbon-based electrocatalysis for hydrogen evolution reactions: A review, Materials Today Sustainability, 2023, https://doi.org/10.1016/j.mtsust.2023.100371.

- [17] Shinagawa, T., Garcia-Esparza, A. T., & Takanabe, K. (2015). Insight on Tafel slopes from a microkinetic analysis of aqueous electrocatalysis for energy conversion. *Scientific Reports*, 5, 13801. https://doi.org/10.1038/srep13801
- [18] Kang, Kevin & Fuller, Jack & Reath, Alexander & Ziller, Joseph & Alexandrova, Anastassia & Yang, Jenny. (2019). Installation of Internal Electric Fields by Non-Redox Active Cations in Transition Metal Complexes. Chemical Science. 10. 10.1039/C9SC02870F.
- [19] Zhang, B., Zheng, X., Voznyy, O., Comin, R., Bajdich, M., Garcia-Melchor, M., ... & Sargent, E. H. (2016). Homogeneously dispersed multimetal oxygen-evolving catalysts. *Science*, 352(6283), 333–337. https://doi.org/10.1126/science.aaf1525
- [20] (For Figure 1) Wahl, Amelie & Dawson, Karen & Sassiat, N & Quinn, Aidan & O'Riordan, Alan. (2011). Nanomolar Trace Metal Analysis of Copper at Gold Microband Arrays. Journal of Physics: Conference Series. 307. 012061.
- 10.1088/1742-6596/307/1/012061.
- [21] Joya, K. S. (2015). In situ Raman and surface-enhanced Raman spectroscopy on working electrodes: spectroelectrochemical characterization of water oxidation electrocatalysts. *Physical Chemistry Chemical Physics*.
- [22] Kim, Hyung. (2015). Endoscopic Raman Spectroscopy for Molecular Fingerprinting of Gastric Cancer: Principle to Implementation. BioMed Research International. 2015. 1-9. 10.1155/2015/670121.
- [23] Mestl, Gerhard. (2000). In Situ Raman Spectroscopy A Valuable Tool to Understand Operating Catalysts. Journal of Molecular Catalysis A: Chemical. 158. 45-65. 10.1016/S1381-1169(00)00042-X.
- [24] Isaac K. Attatsi, Weihua Zhu, Xu Liang, Surface functionalized gold electrode by axial ligand exchanged CoIIIcorroles for accelerating electrocatalyzed hydrogen evolutions, International Journal of Hydrogen Energy, 2022,
- https://doi.org/10.1016/j.ijhydene.2022.03.059.
- [25] Rodriguez, P., & Koper, M. T. M. (2014). Electrocatalysis on gold. *Physical Chemistry Chemical Physics*, 16(27), 13583–13594. https://doi.org/10.1039/c4cp00394b
- [26] Yang, S., & Hetterscheid, D. G. H. (2020b). Redefinition of the active species and the mechanism of the oxygen evolution reaction on gold oxide. *ACS Catalysis*, 10(21), 12582–12589. https://doi.org/10.1021/acscatal.0c03548
- [28] Xia, SJ & Birss, VI. (2001). A multi-technique study of compact and hydrous Au oxide growth in 0.1 M sulfuric acid solutions. ELSEVIER Journal of Electroanalytical Chemistry. 500. 562-573. 10.1016/S0022-0728(00)00415-0.
- [29] Cherevko, S., Zeradjanin, A. R., Keeley, G. P., & Mayrhofer, K. J. J. (2014). A comparative study on gold and platinum dissolution in acidic and alkaline media. *Journal of the Electrochemical Society*, 161(12), H822–H830. https://doi.org/10.1149/2.0881412jes [30] C. McGill, PROCESS ANALYSIS | Overview, Editor(s): Paul Worsfold, Alan Townshend, Colin Poole, Encyclopedia of Analytical Science (Second Edition), 2005, https://doi.org/10.1016/B0-12-369397-7/00485-4.

- [31] Holze, R. (2002). Buchbesprechung: Electrochemical Methods. Fundamentals and Applications. Von Allen J. Bard und Larry R. Faulkner. *Angewandte Chemie*, 114(4), 677–680. https://doi.org/10.1002/1521-3757(20020215)114:4
- [32] standard electrode potential, E°. (2008). In *International Union of Pure and Applied Chemistry (IUPAC) eBooks*. https://doi.org/10.1351/goldbook.s05912
- [33] Groß, A. (2022). Reversible vs Standard Hydrogen Electrode Scale in Interfacial Electrochemistry from a Theoretician's Atomistic Point of View. *The Journal of Physical Chemistry C*, 126(28), 11439–11446. https://doi.org/10.1021/acs.jpcc.2c02734
- [34] P. Sebastián, V. Climent, J.M. Feliu, E. Gómez, Ionic Liquids in the Field of Metal Electrodeposition, 2018, Pages 690-700, ISBN 9780128098943, https://doi.org/10.1016/B978-0-12-409547-2.13379-7.
- [35] Bhattacharyya, K., & Auer, A. A. (2022). Oxygen Evolution Reaction Electrocatalysis on Cobalt(oxy)hydroxide: Role of Fe Impurities. *The Journal of Physical Chemistry C*, 126(44), 18623–18635. https://doi.org/10.1021/acs.jpcc.2c06436
- [36] Zhang, S. (n.d.). In situ raman investigation of the phase transition of NAVO2F2 under variable temperature conditions. *Royal Society of Chemistry*. https://doi.org/10.1039/d1ra02827h
- [37] Yoo, R. M. S., Yesudoss, D., Johnson, D., & Djire, A. (2023). A review on the application of In-Situ Raman spectroelectrochemistry to understand the mechanisms of hydrogen evolution reaction. *ACS Catalysis*, *13*(16), 10570–10601.
- https://doi.org/10.1021/acscatal.3c01687
- [38] Hyeon Seok Lee, Heejong Shin, Subin Park, Jiheon Kim, Euiyeon Jung, Wonchan Hwang, Electrochemically generated electrophilic peroxo species accelerates alkaline oxygen evolution reaction, 2023, 1902-1919, https://doi.org/10.1016/j.joule.2023.06.018. [39] Das, Abhinaba & Mohapatra, Bapuji & Kamboj, Vipin & Ranjan, Chinmoy. (2021). Promotion of Electrochemical Water Oxidation Activity of Au Supported Cobalt Oxide upon Addition of Cr: Insights using in situ Raman Spectroscopy. ChemCatChem. 13. 10.1002/cctc.202001889.
- [40] Sun, X., Xu, K., Fleischer, C., Liu, X., Grandcolas, M., Strandbakke, R., Bjørheim, T. S., Norby, T., & Chatzitakis, A. (2018). Earth-Abundant electrocatalysts in proton exchange membrane electrolyzers. *Catalysts*, 8(12), 657. https://doi.org/10.3390/catal8120657
- [41] Wang, J., Zhang, H., Wang, Z., & Zhou, J. (2021). Recent progress in stability evaluation of electrocatalysts for oxygen evolution reaction. Journal of Energy Chemistry, 56, 377–391. https://doi.org/10.1016/j.jechem.2020.08.010
- [42] Yeo, B. S., & Bell, A. T. (2011). Enhanced activity of Gold-Supported cobalt oxide for the electrochemical evolution of oxygen. *Journal of the American Chemical Society*, 133(14), 5587–5593. https://doi.org/10.1021/ja200559j
- [43] Flis-Kabulska, Iwona. (2006). Electrodeposition of cobalt on gold during voltammetric cycling. Journal of Applied Electrochemistry. 36. 131-137. 10.1007/s10800-005-9024-8.
- [44] Zhou et al., JACS Au, 2021 Direct spectroscopic observation of OOH intermediates in Co-based OER catalysts, https://pubs.acs.org/doi/10.1021/jacsau.1c00346

- [45] Zhang et al., Chem. Soc. Rev., 2021-Instability of Pt-based catalysts in alkaline conditions, https://pubs.rsc.org/en/content/articlelanding/2021/cs/d0cs00930k
- [46] Zhao et al., ACS Catalysis, 2019 Pt dissolution and oxide instability under OER conditions, https://pubs.acs.org/doi/10.1021/acscatal.9b02398
- [47] Buttler, A. & Spliethoff, H. Current status of water electrolysis for energy storage, grid balancing and sector coupling via power-to-gas and power-to-liquids: A review. Renewable and Sustainable Energy Reviews, 82 (2018): 2440–2454. 10.1016/j.rser.2017.09.003

7 Appendix Material

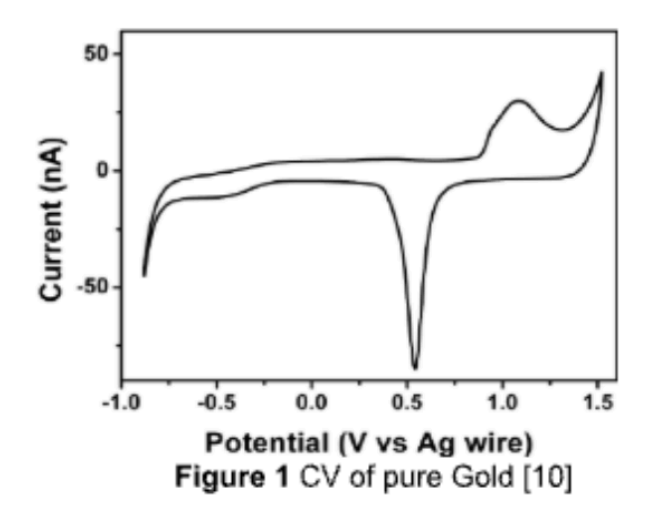
Appendix A

A.1 Definition of Reversible Hydrogen Electrode

The Reversible Hydrogen Electrode (RHE) is a pH-dependent reference electrode whose potential is defined by the equilibrium of the hydrogen redox couple $(2H^+ + 2e^- \rightleftharpoons H_2)$ under standard conditions, making it ideal for comparing electrochemical reactions across different pH environments [33]

A.2 Definitions of CV, LSV, Faradaic efficiency

Cyclic Voltammetry (CV) is used to assess the redox behavior of the catalyst material and to estimate the electrochemical surface area, which correlates with the number of available active sites. [17] CV provides insight into reversible or irreversible surface reactions and the presence of active redox couples (Ni²⁺/Ni³⁺). [18]



Linear Sweep Voltammetry (LSV) is useful for measuring the onset potential, which is the minimum voltage at which the reaction begins, and for recording current density [17].

Faradaic efficiency quantifies the efficiency with which electrons supplied to the system are converted into the desired chemical product. [19].

Chronoamperometry (CA) is an electrochemical technique used to evaluate the stability and durability of a catalyst under constant potential over time. By applying a fixed voltage and measuring the resulting current, CA provides insight into how the catalytic activity evolves during prolonged operation. A steady current response typically indicates good electrochemical stability and resistance to degradation, while a significant drop in current may suggest surface deactivation, dissolution, or structural changes in the catalyst. In the context of oxygen evolution reaction (OER) studies, chronoamperometry helps assess whether the catalyst can sustain water oxidation without losing activity, making it a critical

method for validating long-term performance. Additionally, it can reveal dynamic surface processes such as restructuring or intermediate formation that occur under operating conditions [41].

Appendix B

B.1 Detail on Raman Spectroscopy

The components of a Raman system include a laser source emitting monochromatic light, optical filters to eliminate elastically scattered light, a spectrometer that disperses the Raman-shifted light, and a CCD detector that records the intensity of scattered photons as a function of energy shift. [24] When combined with an electrochemical cell, Raman spectroscopy becomes a powerful tool for correlating electrochemical behavior with molecular-level structural changes, helping to guide the rational design and optimization of next-generation electrocatalysts. [23, 24]

Appendix C

C.1 Detail on Tafel analysis

Tafel analysis is a widely used electrochemical technique to evaluate the kinetics of electrode reactions, particularly for oxygen evolution (OER) and hydrogen evolution reactions (HER). It provides insight into the rate-determining step, mechanism, and electrocatalytic activity of a material. A Tafel plot is a graph of: $\eta = a + b \log i$ Where η is overpotential, i is current density, a is exchange current intercept, b is Tafel slope

C.2 Tafel data from CA

E (V vs RHE)	j (mAcm ⁻²)	$\eta = E - 1.23 \text{ (V)}$	log(j)
1.45	0.02634	0.22	-1.57939
1.49	0.05568	0.26	-1.2543
1.53	0.22214	0.30	-0.65337
1.57	1.05012	0.34	0.02124
1.61	4.44628	0.38	0.648

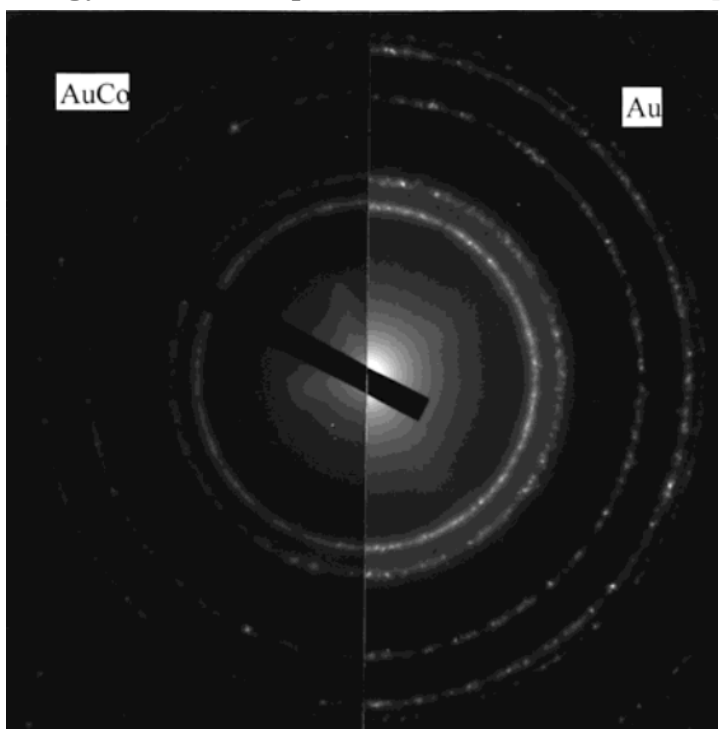
Table 2 CA data to calculate Tafel slope for Au-Co catalyst

E (V vs RHE)	j (mAcm ⁻²)	$\eta = E - 1.23 \text{ (V)}$	log(j)
2.12	2.262	0.89	0.4169
2.16	3.281	0.93	0.5160
2.20	6.477	0.97	0.8114
2.24	14.75	1.01	1.1688
2.28	28.69	1.05	1.0504

Table 2 CA data to calculate Tafel slope for Au catalyst

Appendix E

E.1 Surface morphology of electrodeposited Co on Au substrate [43]



Photograph of Debye-Scherrer rings of electron diffraction of the transition metals and Au. The surface of annealed Au was characterised by flat terraces with about 0.5-nm high steps. At $E=E^{\circ}_{Co/Co2+}$, bright spots appeared on the surface (Figure 9(b)), which are interpreted as islands of electrodeposited Co. They were about 0.5 nm high and 50 nm wide. Similar to the STM results of Figure 6(b), AFM suggests that at low potentials the electrodeposition of Co occurs in the form of islands.